

## Advancing ERW Efficiency: Developing High-Performance Water-Based Mud with Friction Reducer and Precision Prediction for ECD and Open Hole Extension Limits using Herschel-Bulkley Rheological Model

Mohamed Metwally\*

Petroleum Engineering Department, New Mexico Institute of Mining and Technology, New Mexico state, USA

**Citation:** Metwally M. Advancing ERW Efficiency: Developing High-Performance Water-Based Mud with Friction Reducer and Precision Prediction for ECD and Open Hole Extension Limits using Herschel-Bulkley Rheological Model. *J Petro Chem Eng* 2025;1(1): 04-14.

**Received:** 12 January, 2025; **Accepted:** 21 January, 2025; **Published:** 23 January, 2025

\***Corresponding author:** Mohamed Metwally, Petroleum Engineering Department, New Mexico Institute of Mining and Technology, New Mexico state, USA, Email: mohamed.metwally@student.nmt.edu

**Copyright:** © 2025 Metwally M, This is an open-access article published in *J Petro Chem Eng* (JPCE) and distributed under the terms of the Creative Commons Attribution License, which permits unrestricted use, distribution, and reproduction in any medium, provided the original author and source are credited.

### ABSTRACT

Drilling horizontal and extended reach wells (ERW) plays pivotal role to increase well productivity, achieve efficient reservoir drainage, reduce environmental impact, and mitigate water coning production problem. The continuous improvements in horizontal drilling and completion technology have prompted operators to consistently seek the drilling of longer lateral wells, aiming to more hydrocarbon production. Nevertheless, there are technical drilling operational challenges that limit extension of lateral horizontal section such as high torque and drag, shale instability, limited surface pump capacity, and the increase of equivalent circulation density (ECD) within a narrow mud window, situated between pore pressure and fracture pressure. This paper focuses on overcoming these technical problems by developing high performance water-based mud (WBM) using friction reducer (FR) to drill ERW in shaly Wolfcamp formation with Permian basin. The design consideration for the developed WBM are inhibition shale instability problems, reducing ECD, and approaching performance of oil-based mud (OBM), and increasing open hole extension limit for ERW.

The objectives of this study are: (1) to develop experimentally high performance WBM using FR to prevent shale swelling and dispersion, and approach OBM performance in terms of thermal stability; (2) to develop WBM to decrease both ECD and surface pump pressure; and (3) to couple hydraulic Herschel-Bulkley rheological model with fracture pressure to determine maximum open hole extended limit for ERW.

The lab results reveals that the developed WBM has thermal stability withing Wolfcamp formation's temperature conditions. Besides, adding FR to WBM stabilize clay surface, enhances shale inhibition, and prevent clay water interactions. Moreover, the model presented in this paper using Herschel-Bulkley rheological parameters provides accurate predictions for ECD. According to the case analysis calculation, the hydraulic model proved the formulated WBM with FR has the same ECD as OBM in ERW at different measured depth. The coupled hydraulic Herschel-Bulkley rheological model with fracture pressure show increase in drilling open hole extended limit when FR is used in WBM to drill ERW in shaly Wolfcamp formation within Permian basin.

This study introduces a developed high-performance WBM designed to reduce pressure loss, mitigate shale swelling, and serve as a substitute for OBM in drilling ERW in the Permian Basin. Additionally, it offers a robust model for predicting ECD and increasing the open-hole extension limit based on a safe mud weight window to enhance wellbore stability.

## 1. Introduction

Drilling horizontal and Extended Reach Wells (ERW) maximizes contact with the reservoir compared to vertical wells. The increased reservoir contact often leads to higher well productivity<sup>1</sup>. This is especially beneficial in situations where the reservoir has low permeability or is challenging to produce using vertical wells. Besides, the horizontal wells and ERW reduce number of production wells. Drilling fewer wells to access the same or larger reservoir volumes can reduce the environmental footprint<sup>2</sup>. Additionally, drilling horizontal wells and ERW proves beneficial for efficiently draining reservoirs and serves as a method to mitigate water coning, particularly in reservoirs characterized by thin oil columns and a robust active bottom-water drive<sup>3</sup>.

ERW in drilling industry is defined when the ratio between Measured displacement (MD) and true vertical depth (TVD) is higher than 2<sup>4</sup>. The envelope for ERW has been steadily expanding in recent years, and currently it is common to drill ERWs with MD to TVD ratios larger than 6<sup>5</sup>. The current world record for the longest measured depth for ERW is the Chayvo Z-42 well (Exxon Neftegaz Limited, Sakhalin Island, Russia) with MD of 41,667 ft. and horizontal section of 38,514 ft<sup>6</sup>. Advancements and enhancements in horizontal drilling and completion technology have led operators to consistently pursue the drilling of increasingly longer lateral wells to amplify hydrocarbon production<sup>7</sup>.

Efficient drilling of ERW in shortest time holds significant importance, contributing to drilling safety, minimizing reservoir damage, and optimizing efficiency and economic returns<sup>8</sup>. But the drilling of ERW is restricted by extension limit of the horizontal section. The open hole extension limit of ERW mainly depends on formation fracture pressure, annular pressure losses, and equivalent circulation density (ECD) of drilling fluid<sup>9</sup>. From the perspective of drilling fluids, there are technical operational challenges linked with ERW commonly encompass the following issues: hole cleaning, drilling in narrow window between pore pressure and fracture pressure, shale instability problems, and torque and drag<sup>10</sup>. Regarding hole cleaning in ERW, there is a demand for a higher circulation rate for better hole cleaning, and this is constrained by the limitations in surface pumping capacity. The higher circulation rate can finally lead to increase ECD and limit open hole extension for ERW<sup>11</sup>. Therefore, drilling fluid plays significant role to drill successfully, safety, and economically the ERW. Drilling fluids can be categorized into two types, depending on the continuous phase: Water-based fluids (WBM) and Oil based mud (OBM).

Generally, OBM is drilling fluid of choice to drill horizontal wells and ERW<sup>12</sup>. OBM has advantages to improve the rate of penetration, enhance the thermal stability of rheology, elevate lubricity, reduce the coefficient of friction during the drilling of horizontal wells and ERW, prevent swelling and dispersion of shale formations, and enhance wellbore stabilization<sup>13</sup>. On the other hand, Environmental Protection Agency (EPA) set regulations for limiting use of OBM due to its detrimental effect on the environment. Besides OBM has disadvantages such as high cost, disposal problems, and health and safety issues<sup>14</sup>. Therefore, the current ever increasing environmental legislations in preventing OBM application in the industries have dictated the use of WBM as the most environmentally acceptable alternative. The industry's movement towards clean, sustainable well-site practices coupled with longer lateral intervals, along with a demand to stabilize shale.

While WBM is being environmentally friendly, it has big concern in drilling shale formation. As, using conventional WBM to drill shale formations can pose several challenges due to the unique characteristics of shale. As, shale formations often contain clays that can swell and disperse in contact with water. Conventional WBM may not adequately inhibit clay swelling and dispersion, leading to wellbore instability, increased torque and drag, and potential stuck pipe issues<sup>15</sup>. Besides, shale formations generate fine and sticky cuttings that can be challenging to disperse and transport effectively to the surface. Inadequate cuttings removal can result in bit balling, poor hole cleaning, and potential for equipment damage. Moreover, shale formations may react chemically with water-based mud components, affecting the mud properties and causing formation damage. The interaction between the shale and the mud can result in issues such as increased mud weight, and reduced fluid loss control. In addition to that, shale formations can undergo significant volume changes, causing hole enlargement issues when using conventional WBM. This can lead to difficulties in cementing operations and may require additional casing sizes to address the enlarged borehole<sup>16</sup>.

Hence, oil industry has tried over the years to develop WBM to approach performance of OBM for drilling ERW. The key parameter for this development is shale inhibition. The developed WBM is called high performance WBM<sup>17</sup>. While high-performance WBM has the potential to stabilize shale and prevent wellbore instability issues in drilling ERW, the primary concern arises from the increase of annular pressure loss associated with the required a high circulation rate to enhance hole cleaning.

Because high pumping circulation rate causes turbulence, leads to notable energy loss and increased hydraulic friction. To mitigate the challenges posed by elevated frictional resistance and reduce pumping discharge, there is a growing emphasis in the petroleum industry on using friction reducer (FR) agents<sup>18</sup>. Polymeric FRs are linear polymers with high molecular weights that can lower frictional pressure loss in turbulent flow when being added in low concentrations<sup>19</sup>. There are many applications for polymeric FR such as oil transportation, irrigation, firefighting, building heating, transportation of drinking water and wastewater and hydraulic fracturing<sup>20-24</sup>. The main function of polymeric FR in the mentioned applications is the pressure loss reduction.

In elucidating the mechanism by which polymer FR mitigates pressure loss, Bradshaw<sup>25</sup> introduced the Prandtl Mixing Length theory. This theory classifies the velocity cross-section profile within the pipe into two layers in the absence of FR, as illustrated in (**Figure 1a**): the first layer is the viscous sub-layer, situated at the pipe boundary, where the flow is laminar, resulting in lower pressure loss. The second layer is the inertial layer, located at the pipe center, characterized by turbulent flow with fluctuations and eddies primarily in the radial direction. The major pressure losses occur in the inertial layer, leading to an increase in pressure loss with higher flow rates<sup>26</sup>.

Conversely, in the presence of polymer FR, Bradshaw<sup>25</sup> divides the cross-sectional velocity profile into three layers: the viscous sub-layer, inertial layer, and elastic buffer layer, as depicted in (**Figure 1b**). The newly formed buffer layer emerges between the viscous sub-layer and the inertial layer. Diamond<sup>27</sup> noted that when FR uncoils and stretches in the flow, it alters the flow fluctuations from the radial direction to the axial direction within the buffer layer, resulting in laminar flow. As this buffer

layer expands toward the pipe center, the inertial layer contracts, leading to an enhancement in drag reduction.

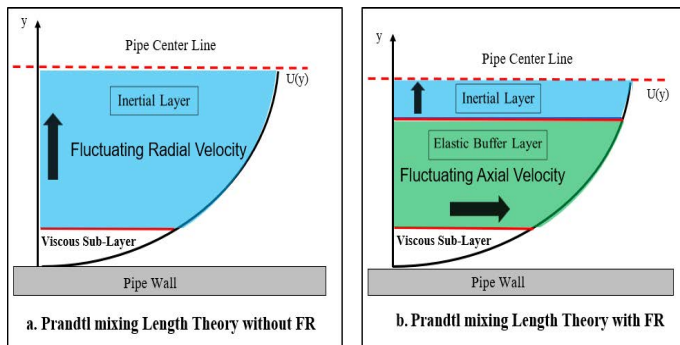


**Figure 1:** Mechanism of friction reduction by using polymeric friction reducer (FR).

Adding FR in WBM may be a solution to reduce friction pressure loss in drilling ERW. Besides, the available FR in the paper is emulsified polyacrylamide base, this may be used as a shale inhibitor to stabilize clay. In this study, FR will be used to formulate WBM to drill horizontal well and ERW in shaly Wolfcamp formation in the Permian basin. As, the Permian basin is considered as one of the most prolific oil and gas-producing regions in USA<sup>28</sup>. The Wolfcamp Formation within Permian basin is recognized as the foremost unconventional oil source in the United States because it consists of organic shale and carbonates with substantial clay mineral content. The temperature range of Wolfcamp formations within the Permian Basin spans from 130° F to 180° F<sup>29</sup>. Currently, due to advancements in horizontal drilling technology, the proportion of horizontal wells within the Wolfcamp Formation stands at 90%, a significant surge compared to the mere 4% represented by vertical wells<sup>30</sup>. Hence, developing high performance WBM to extend ERW horizontal section in Wolfcamp formations contributes to the further development of development of this prolific hydrocarbon-bearing formation.

## 2. Objective

The target of this paper is to develop high performance WBM using FR to approach OBM performance. The developed WBM is designed for drilling ERW in the shaly Wolfcamp formation within the Permian Basin. The evaluations of the high-performance WBM involve measuring fluid rheology, fluid loss, and testing shale inhibition capabilities. Additionally, an ancillary objective is to establish a modified openhole extended reach limit model using the Herschel-Bulkley rheological model to calculate ECD and determine the maximum horizontal section limit for ERW when employing the developed WBM, which is then compared with OBM.

## 3. Methodology

This study represents a comprehensive investigation that integrates both experimental measurements and modeling to enhance the depth of understanding in the targeted research area. The experimental aspect of the research adhered to the guidelines and recommendations set forth by the American Petroleum Institute (API).

### 3.1 The Experimental Part

#### 3.1.1 Materials

(Table 1) demonstrates basic additives used to formulate the testing fluids of WBM with its function.

**Table 1:** Additives used to formulate WBM samples and its corresponding functions.

#	Additives	Function
1	Bentonite	provide initial viscosity, suspension, and fluid loss control
2	caustic soda	Control pH
3	Starch and PAC-L	provide fluid loss reduction
4	Xanthan Gum (XC) polymer	Control viscosity
5	Potassium chloride salt (KCl)	use for shale inhibition purpose
6	Barite control	drilling fluid density

The supposed main additive to formulate high performance WBM in this study is FR, which is a commercial liquid polymer product that was provided from Chemplex Solvay Company. This FR has been originally used in hydraulic fracture job to reduce frictional pressure loss. It is acrylamide base polymer which was synthesized using emulsion polymerization with density of 9.09 ppg.

#### 3.1.2 Preparation of Drilling Mud Samples

Basic WBM was formulated by using fresh water, bentonite, caustic soda, starch, PAC-L, XC polymer, and barite. The composition of different drilling WBMs, mixing time, additives concentration is given in (Table 2).

**Table 2:** Formulation of different WBMs with FR.

Additives	Mixing Time, Min	Basic WBM	WBM 1	WBM 2
Fresh water, bbl	-	1	1	1
Bentonite, Lb	10	8	8	8
caustic soda, Lb		0.15	0.15	0.15
FR, Lb	5	0	0.25	0.5
Starch, Lb	10	3	3	3
PAC-L, Lb	10	1	1	1
XC polymer, Lb	10	0.75	0.75	0.75
KCl salt, Lb	10	17.5	17.5	17.5
Barite, Lb	20	As required	As required	As required

#### 3.1.3 Experimental Apparatus

The experimental work is essential for evaluating the developed high performance WBM to drill ERW in shaly Wolfcamp formation within Permian basin. This evaluation is based on measuring fluid rheology, fluid loss, and determination shale inhibition of the formulated WBM.

The fluid rheology was measured using OFITE 900 viscometer. As, the OFITE 900 viscometer measured automatically shear stress versus different shear speeds at different temperatures up to 200° F and ambient pressure. OFITE Roller oven was used to simulate the drilling fluid inside the well as drilling fluid sample was put in a cell and rotated in the oven at any specific temperature. This oven has 5 rollers, and the aging can be done under static or dynamic conditions from ambient temperature up to 600° F. Fluid loss was measured by both API filter press, and HPHT filter press using API technical procedures. The API fluid loss is measured at ambient temperature and 100 psi. While HPHT fluid loss is measured at 250 °F and 500 psi<sup>31</sup>.

According to shale inhibition purpose, there are many techniques to test and evaluate shale inhibitor performance in WBM. These techniques are zeta potential, linear swelling test, hot rolling dispersion test, capillary suction test, methylene blue

test, and scanning electron microscope<sup>32</sup>. Zeta potential, shale dispersion test, were used in this study for study shale inhibition.

Shale dispersion test is also known as cutting dispersion test. The clay cuttings are ground and sieved by 20-30 mesh screens. The weighted sieved clay cuttings are placed in the aging cell with the formulated drilling fluid in the roller oven for 16 hrs. Then shale cuttings are washed and recovered by sieve of 50 mesh. After that, the recovered shale cuttings are heated again in the roller oven for 3 hrs to make sure all water is evaporated. Finally, the recovered shale after heating over the original shale weight is indication of shale recovery percentage. Clearly, higher shale recovery means better shale fluid inhibitor<sup>33</sup>.

$$\text{Shale Recovery} = \frac{\text{dry recovered shale cuttings from mud}}{\text{Initial weight of shale cuttings}} \times 100 \quad (1)$$

Zeta potential is another method to evaluate shale stabilization. Zeta potential is measured by electrophoretic light scattering. Zeta potential is powerful tool to give indication about attraction and repulsion. When zeta potential has small value than absolute value of 20 mV, this means the tested fluid has capability to prevent shale swelling and shale dispersion<sup>34</sup>. The measurement of zeta potential through electrophoretic light scattering was conducted using the Litesizer 500, a product manufactured by Anton Paar. In this study, test samples were prepared by blending chemical additives with water, and their pH values were manually adjusted using a pH meter. To prevent the entrapment of air bubbles, the samples were loaded into an omega cuvette using an inversion method. Water, serving as the base fluid for all formulations, was used as the solvent. The samples were allowed to equilibrate for 3 minutes within a temperature range of 0 to 90°C, and zeta potential for the fluid sample can be easily measured.

### 3.2 The Modeling Part

The modeling part in this study is based on mud hydraulics using the Herschel-Bulkley model to predict annular pressure loss, and ECD. The model to predict open hole extension limit is based on pore pressure, fracture pressure, and annular friction pressure losses with following the assumptions:

- The Herschel-Bulkley model is used to simulate mud rheology and predict hydraulic annular pressure losses.
- The eccentricity of drill string is considered in the large inclination and horizontal sections.
- The well is in an ideal borehole cleaning state; hence the effect of cuttings on the annular pressure is not considered.
- Effect of pipe rotation is not considered.

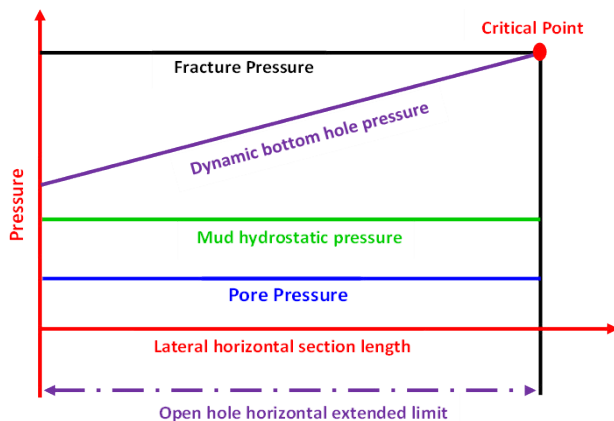


Figure 2: Schematic overview of the horizontal-section limit.

ECD is critical term in drilling operation and depends on annular pressure loss. But open hole extended reach wells depend on both annular pressure drop and fracture pressure of the drilled formation. Deli<sup>35</sup> proposed the first concept of open hole extended limit for horizontal well. His concept mentioned the ERW cannot be further extended stopped when dynamic bottom hole pressure or mud circulation pressure ( $P_{bh}$ ) is equal to fracture pressure ( $P_f$ ), which is considered as a critical point as illustrated in figure 1. Mathematically at critical point, the summation of hydrostatic pressure ( $P_{hy}$ ) and annular pressure loss ( $\Delta P_a$ ) for all drilled sections is equal to fracture formation pressure as expressed in Eqs (2-5).

$$P_{bh} = P_f \quad (2)$$

$$P_{hy} + \Delta P_a = P_f \quad (3)$$

$$0.052\rho_m L_v + \Delta P_a = 0.052\rho_f L_v \quad (4)$$

$$0.052\rho_m L_v + (\Delta P_v + \sum \Delta P_d + \Delta P_h) = 0.052\rho_f L_v \quad (5)$$

Where,  $\rho_m$  is the drilling fluid density in ppg,  $L_v$  is the true vertical depth in ft, and ( $\Delta P_v$ ,  $\sum \Delta P_d$ ,  $\Delta P_h$ ) are the pressure losses in psi which located in vertical, deviated, horizontal sections, respectively.

By rearranging Eq. (5), the maximum allowable annular pressure loss in horizontal section can be obtained using Eq. (6). The open hole horizontal section limit ( $L_h$ ) in ERW can be obtained using Eq. (7) if the pressure loss gradient in horizontal section has been calculated.

$$\Delta P_h = 0.052(\rho_f - \rho_m)L_v - (\Delta P_v + \sum \Delta P_d) \quad (6)$$

$$L_h = \frac{\Delta P_h}{(\Delta P / \Delta L)_h} \quad (7)$$

Pressure Loss Calculations Based on Herschel-Bulkley Rheological Model

The Herschel-Bulkley model predicts and correctly simulates the drilling fluid rheology better than the Bingham plastic and the power law rheological models<sup>36</sup>. Therefore, Herschel-Bulkley model is used to calculate annular pressure loss and the ECD.  $\tau_y$  is the shear stress measured at shear rate of 0.1 S<sup>-1</sup> using OFITE 900 viscometer. The Herschel-Bulkley model parameters (K and n) will be calculated using regression analysis as expressed in Eq. (9) and Eq. (10).

$$\tau = \tau_y + K\gamma^n \quad (8)$$

Where:  $\tau_y$  is yield stress (lb/100 ft<sup>2</sup>), n is flow behavior index, K is Flow consistency index ((lb. S<sup>n</sup>/100 ft<sup>2</sup>),  $\tau$  is shear stress (lb/100 ft<sup>2</sup>), and  $\gamma$  is the shear rate (S<sup>-1</sup>).

$$n = \frac{\sum \log(\tau - \tau_y) \sum \log(\gamma) - N \sum (\log(\tau - \tau_y) \log(\gamma))}{(\sum \log \gamma)^2 - N \sum (\log \gamma)^2} \quad (9)$$

$$\log(K) = \frac{\sum \log(\tau - \tau_y) - n \sum \log(\gamma)}{N} \quad (10)$$

Annular pressure loss calculations depend on flow regime: if the flow is laminar or turbulent. Reynolds number ( $N_{Re}$ ) and critical Reynolds number ( $N_{Rec}$ ) are used to determine flow regime using Herschel-Bulkley model as seen in Eqs. (12) and (14)<sup>37</sup>.

$$v = \frac{q}{2.448(d_o^2 - d_i^2)} \quad (11)$$

Where:  $v$  is the average fluid velocity in the annulus,  $q$  is

pump flow rate in gpm, and  $d$  is diameter in inch. The subscripts  $i$  and  $o$  are for inner and outer, respectively.

$$N_{Re} = \frac{4(2n+1)}{n} \left[ \frac{\rho v^{(2-n)} \left(\frac{d_o - d_i}{2}\right)^n}{\tau_y \left(\frac{d_o - d_i}{2v}\right)^n + K \left(\frac{2(2+1)}{nC_a^*}\right)^n} \right] \quad (12)$$

$$C_a^* = 1 - \left(\frac{1}{n+1}\right) \frac{\tau_y}{\tau_y + K \left\{ \frac{2q(2n+1)}{n\pi \left[\frac{d_o}{2} - \frac{d_i}{2}\right]^2 \left[\left(\frac{d_o}{2}\right)^2 - \left(\frac{d_i}{2}\right)^2\right]} \right\}} \quad (13)$$

$$N_{Rec} = \left[ \frac{8(2n+1)}{ny} \right]^{\frac{1}{1-z}} \quad (14)$$

$$y = \frac{\log(n) + 3 \cdot 93}{50} \quad (15)$$

$$z = \frac{1 \cdot 75 - \log(n)}{7} \quad (16)$$

In equations 11 and 12, the flow rate ( $q$ ) is in  $\text{ft}^3/\text{s}$ , the  $d_i$  and  $d_o$  are in  $\text{ft}$ , and the fluid density( $\rho$ ) is in  $\text{lb}/\text{ft}^3$ .

If  $N_{Re} < N_{Rec}$ , then the flow is laminar, and the annular pressure loss gradient is calculated using Eq. (17).

If  $N_{Re} > N_{Rec}$ , the flow is turbulent, and the annular pressure loss gradient is calculated using Eq.(18).

$$\frac{\Delta P}{\Delta L} = \frac{f_a q^2 \rho_m}{1421 \cdot 22(d_o - d_i)(d_o^2 - d_i^2)^2} \quad (18)$$

$$f_a = y(C_a^* \cdot N_{Re})^{-z} \quad (19)$$

In this paper, the horizontal ERW is categorized into two section types: the vertical and small inclination sections, and the large-inclination and horizontal sections. The vertical section and the small inclination section exhibit an inclination range of  $0^\circ$  to  $30^\circ$ , while the large-inclination section has an inclination range extending from  $30^\circ$  to  $90^\circ$ <sup>38</sup>. The annular pressure drops  $\Delta P_V$ ,  $\Delta P_{dS}$  of the vertical and small inclination section, respectively, can be expressed using Eqs. 20, and 21.  $\Delta L$  will be replaced by  $L_V$  and  $L_{dS}$ , the vertical and small inclination section, respectively.

If the flow is laminar

$$\Delta P = \frac{4K}{14400(d_o - d_i)} \left\{ \left(\frac{\tau_y}{K}\right) + \left[ \left(\frac{16(2n+1)}{nC_a^*(d_o - d_i)}\right) \left(\frac{q}{\pi(d_o^2 - d_i^2)}\right) \right]^n \right\} \Delta L \quad (20)$$

If the flow is Turbulent

$$\Delta P = \frac{f_a q^2 \rho_m}{1421 \cdot 22(d_o - d_i)(d_o^2 - d_i^2)^2} \Delta L \quad (21)$$

On the other hand, annular pressure loss in the large-inclination section differs from that in the vertical section. In the large-inclination and horizontal sections, the drill string may experience an eccentric state due to gravity, and this eccentricity can significantly impact the annular pressure drop. Therefore, the eccentric coefficient ( $R$ ) is introduced in this context. Bailey and Peden<sup>39</sup> defined eccentric coefficient ( $R$ ) to be ratio between the pressure loss gradients in the eccentric annulus and the pressure loss gradients in the concentric annulus as illustrated in Eq. (22).

$$R = \frac{\left(\frac{\Delta P}{\Delta L}\right)_{ecc}}{\left(\frac{\Delta P}{\Delta L}\right)_{conc}} \quad (22)$$

$R$  is a dimensionless factor and determined according to the flow pattern: laminar eccentric coefficient  $R_{lam}$  and turbulent eccentric coefficient  $R_{turb}$ .  $R_{lam}$  and  $R_{turb}$  are expressed in Eqs. (23) and (24), respectively<sup>39</sup>.

$$R_{lam} = 1 - 0.072 \frac{\varepsilon}{n} \left(\frac{d_i}{d_o}\right)^{0.8454} - \frac{3}{2} \varepsilon^2 \sqrt{n} \left(\frac{d_i}{d_o}\right)^{0.1852} + 0.96 \varepsilon^3 \sqrt{n} \left(\frac{d_i}{d_o}\right)^{0.2527} \quad (23)$$

$$R_{turb} = 1 - 0.048 \frac{\varepsilon}{n} \left(\frac{d_i}{d_o}\right)^{0.8454} - \frac{2}{3} \varepsilon^2 \sqrt{n} \left(\frac{d_i}{d_o}\right)^{0.1852} + 0.285 \varepsilon^3 \sqrt{n} \left(\frac{d_i}{d_o}\right)^{0.2527} \quad (24)$$

Where  $\varepsilon$  is the dimensionless eccentricity. For a concentric annulus,  $\varepsilon$  is equal to 0; while for a completely eccentric annulus,  $\varepsilon$  is equal to 1<sup>40</sup>.

Therefore, annular pressure loss is calculated in long deviation section by using Eqs. (25) and (26).

If the flow is laminar

$$\Delta P = \frac{4K}{14400(d_o - d_i)} \left\{ \left(\frac{\tau_y}{K}\right) + \left[ \left(\frac{16(2n+1)}{nC_a^*(d_o - d_i)}\right) \left(\frac{q}{\pi(d_o^2 - d_i^2)}\right) \right]^n \right\} \Delta L * R_{lam} \quad (25)$$

If the flow is Turbulent,

$$\Delta P = \frac{f_a q^2 \rho}{1421 \cdot 22(d_o - d_i)(d_o^2 - d_i^2)^2} \Delta L * R_{turb} \quad (26)$$

In addition, annular pressure loss gradient for the horizontal section is calculated using Eqs. (27), and (28) by taking the eccentricity factor in the consideration.

If the flow is laminar

$$\left(\frac{\Delta P}{\Delta L}\right)_h = \frac{4K}{14400(d_o - d_i)} \left\{ \left(\frac{\tau_y}{K}\right) + \left[ \left(\frac{16(2n+1)}{nC_a^*(d_o - d_i)}\right) \left(\frac{q}{\pi(d_o^2 - d_i^2)}\right) \right]^n \right\} * R_{lam} \quad (27)$$

If the flow is Turbulent

$$\left(\frac{\Delta P}{\Delta L}\right)_h = \frac{f_a q^2 \rho}{1421 \cdot 22(d_o - d_i)(d_o^2 - d_i^2)^2} * R_{turb} \quad (28)$$

### 3.2.2 Procedures to Calculate ECD at Specific Measured Depth of Horizontal well

The following steps are used to determine ECD for any drilling fluid at specific measured depth.

1. Calculate average fluid velocity using Eqs. (11) by knowing circulation flow rate.
2. Determine Herschel-Bulkley model parameters  $n$ ,  $K$ , and  $\tau_y$  for used drilling fluid.
3. Calculate the annular pressure drops  $\Delta P_V$  and  $\Delta P_{dS}$  of the vertical section and small-inclination section, respectively, using Eqs. (20) or (21);
4. Calculate the eccentric coefficient  $R$  using Eqs. (23) and (24);
5. Calculate the annular pressure drop  $\Delta P_{dl}$  of the large-inclination section, and annular pressure loss  $\Delta P_h$  of the horizontal section using Eqs. (25) or (26);
6. Calculate the total pressure loss at specific measured depth by summation of  $\Delta P_V$ ,  $\Delta P_{dS}$ ,  $\Delta P_{dl}$ , and  $\Delta P_h$ ;
7. Calculate the ECD in ppg using Eq. (29)

$$ECD = \rho_m + \frac{\text{Total annular pressure losses}}{0.052 \times \text{True verticle depth}} \quad (29)$$

### 3.2.3 Procedures to Determine Open Horizontal Extension Limit

The calculation procedure of the modified model is summarized as follows:

1. Calculate the annular pressure drops  $\Delta P_V$  and  $\Delta P_{dS}$  of the vertical section and small-inclination section, respectively, using Eqs. (20) or (21);

- Calculate the eccentric coefficient  $R$  using Eqs. (23) and (24);
- Calculate the annular pressure drop  $\Delta P_{dl}$  of the large-inclination section using Eq. (25) or (26);
- Calculate the pressure loss gradients in the horizontal section  $(\Delta p/\Delta L)_h$  using Eq. (27) or (28);
- Calculate open hole horizontal extension limit  $l_h$  using Eq. (7)

#### 4. Results and Discussions

The basic WBM in this study is composed of main additives: bentonite, caustic soda, starch, PAC-L, XC polymer, KCl salt, and barite. But the main additive to develop high performance WBM is emulsified polymeric FR. The main function groups in FR are the amide group ( $\text{CONH}_2$ ), carboxylic groups ( $\text{COOH}$ ), and carboxylate group ( $\text{COO}^-$ ), so the current FR is anionic polymer. In the basic medium, carboxylic group ( $\text{COOH}$ ) is ionized to negative carboxylate group ( $\text{COO}^-$ ).

The developed WBM is the fluid that contain FR with the main additives. The first part in this study is to experimentally evaluate the developed WBM for rheology stability and shale inhibition and purposes. To determine thermal stability of the formulated WBM samples, the fluid rheology was measured at different temperatures by using OFITE 900 viscometer.

The shear stress is measured with different shear rate for WBM samples illustrated in (Table 2) at temperature 120°, 150°, and 180° F as shown in (Figures 3, 4, 5). The measurements in (Figure 3) demonstrates that fluid rheology of WBM without FR had thermal degradation as the measured shear stress reduced when temperature increased from 120° F to 180° F. on the other hand, WBM with different FR concentration had higher thermal stability than WBM without FR as seen in (Figures 4, 5). The thermal stability happened due to interaction between FR and bentonite. This interaction occurred by the electrostatic attraction between negative carboxylate group ( $\text{COO}^-$ ) to positive bentonite edge and hydrogen bond formed between amide group on FR surface and hydroxide groups located on bentonite negative surface. This hydrogen bond enhanced when temperature increased<sup>41</sup>. Besides, KCl salt may work as a bridging between negative groups on FR surface and negative bentonite. Therefore, the attractions between FR and bentonite leads to stability in rheology when temperature raised from 120° F to 180° F. Additionally, WBM with FR has high low-end rheology in comparison with WBM without FR. High low-end rheology means high apparent viscosity measured at low shear rates which is essential for carrying drilling cuttings and suspending weighting materials<sup>42</sup>. This indicates the formulated WBM has better suspension for drilling cuttings than WBM without FR.

In terms of fluid loss point of view, both API and HPHT fluid losses were measured to evaluate filtration property of FR. The results are tabulated in (Table 3). Adding FR has minor effect on decreasing both API and HPHT fluid losses as API, and HPHT fluid losses reduced from (7ml to 5.5 ml) and (13 ml to 11 ml), respectively after adding 0.5 lb/bbl FR to WBM. This minor reduction in both API and HPHT fluid losses is due to interactions between FR and bentonite. Although the reduction in both API and HPHT fluid losses is minimal, this will help in reducing formation damage.

**Figure 3:** The mud rheology of formulated WBM without FR.

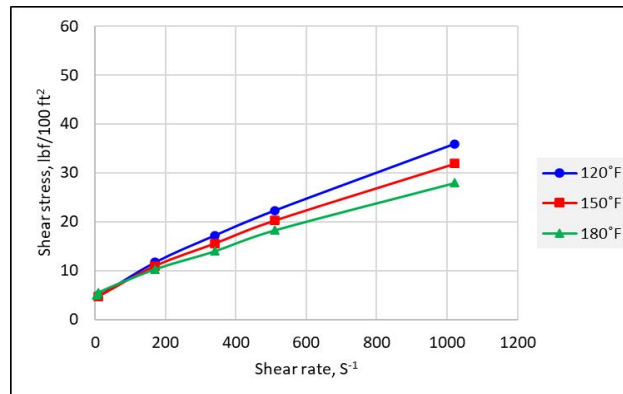


**Table 3:** API and HPHT fluid losses for the formulated WBM with and without AFR.

	W B M without FR	WBM with 0.25 lb/bbl FR	WBM with 0.50 lb/bbl FR
API fluid loss(ml/30 min)	7	6	5.5
HPHT fluid loss at 250° F (ml/30 min)	13	11	11

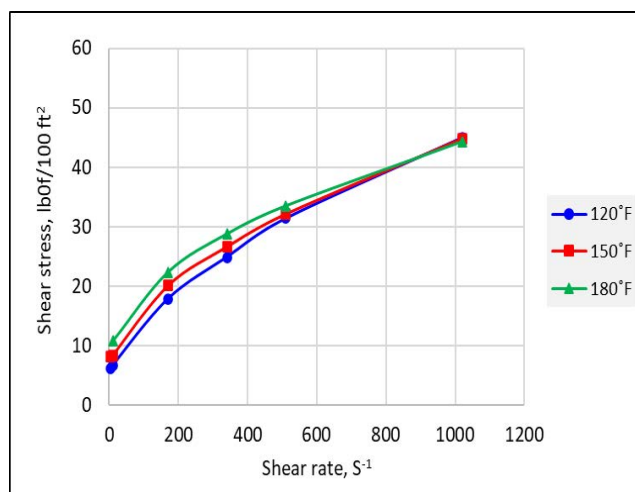


**Figure 4:** The mud rheology of formulated WBM with 0.25 lb/bbl FR.

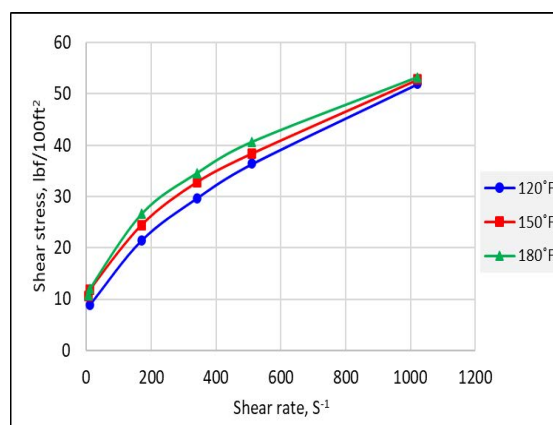


**Figure 5:** The mud rheology of formulated WBM with 0.50 lb/bbl FR

Clearly, FR enhanced fluid rheology of WBM and its thermal stability with minimal effect on filtration property. The target now is to evaluate capability of the developed WBM with FR for shale inhibition. The evaluation is carried out based on shale dispersion test and zeta potential. Dispersion tests were conducted to ascertain the shale recovery percentage when employing a formulated WBM containing 0.25 and 0.50 lb/bbl of FR. The

shale cuttings utilized in the experiment were sourced from the Wolfcamp shaly formation. The outcomes of the shale recovery from dispersion tests are presented in (Table 4). Shale recovery reached 90% and 98% with FR concentrations of 0.25 and 0.50 lb/bbl, respectively in comparison with 60% in case of WBM without FR. This indicates that FR effectively inhibits shale dispersion. The FR prevents water-shale interaction, stabilizes shale, and inhibits both shale swelling and dispersion because of interaction between FR and clay. As there is electrostatic attraction between negative carboxylate groups and positive clay edges. Also, there are hydrogen bonds formed between amid group on FR and negative clay surface. These interaction besides FR being highmolecular weight enable FR to encapsulate the shale or clay surface and prevent water-shale interaction. Consequently, the formulated WBM containing FR demonstrates the capability to inhibit shale swelling and dispersion.

**Table 4:** Results of Shale dispersion test for WBM with and without FR.

Mud Type	Shale Recovery (%)
WBM with 0 lb/bbl FR	60
WBM with 0.25 lb/bbl FR	90
WBM with 0.50 lb/bbl FR	98

Another test conducted to appraise the shale inhibition properties of the developed WBM with FR involved examining the zeta potential. The zeta potential was measured for three distinct samples (bentonite, bentonite with KCl salt, and bentonite with KCl and FR) at various temperatures. Bentonite was used to simulate clay with high swelling tendency. The recorded zeta potential magnitudes for the three samples decreased from (66 mV, 14 mV, 7 mV) to (34 mV, 10 mV, 4 mV), respectively, with a temperature increase from 80°F to 150°F, as represented in Fig.6. Zeta potential measurements validate the attraction between FR and the bentonite surface. Furthermore, the decrease in zeta potential, particularly when FR is introduced to a mixture of bentonite and KCl, substantiates that KCl functions as a bridge connecting the negative  $COO^-$  groups on FR with the negatively charged clay surface. This interaction intensifies the attraction between FR and the shale surface. Consequently, the enhancement of shale inhibition will occur.

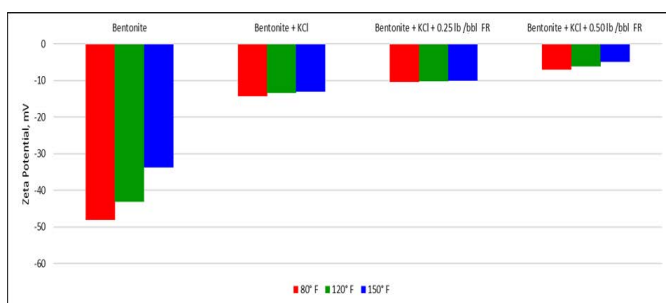


**Figure 6:** Zeta potential for the formulated WBFs with different AFR concentrations.

The developed WBM using FR has ability to prevent shale swelling and shale dispersion. FR can be used a shale inhibitor in WBM. The successful drilling of wells relies on sufficient technical design and the careful selection of drilling fluid with a low ECD. Recently, the design of wellbore has become more complicated. Numerous wells, particularly those in deep water settings, present substantial challenges for the effective management of wellbore pressure. These challenges are evident in the form of a limited margin between pore pressure and fracture gradient. Operations facing such a narrow margin necessitate

enhanced control over ECD to ensure operational efficiency and economic viability. Besides, drilling depleted zones commonly poses a challenge in terms of ECD due to the decline in both pore and fracture pressures<sup>43</sup>. Therefore, calculating ECD before initiating drilling operations is a fundamental practice that contributes to the overall success and safety of the drilling process. Consequently, the author calculated ECD for the developed WBM with FR and compared with OBM for actual well which being drilled in Wolfcamp formation within Permian basin.

There is actual data for horizontal well that was drilled in Wolfcamp formation within Permian basin. This well is used in this study as a case study. The sketch of wellbore and types of drilling fluids used in drilling every section for this well is illustrated in (Figure 7). As seen in Figure 7, the well had total MD of 19270 ft and TVD of 9020 ft. and the deviated and horizontal sections were drilled using OBM with (80/20) oil water ratio at density of 8.75 ppg. The well has small operating mud windows because the pore press equivalent density and fracture pressure equivalent density are 8.4, 10.6 ppg, respectively. The pump flow rate used to drill horizontal section was 846 gpm with 5-inch drill pipe as tabulated in (Table 5).

**Table 5:** Actual Well data for the drilled ERW in the Wolfcamp formation.

Input parameters	Value	Unit
Outside diameter of drill pipe	5	inch
Inside diameter of intermediate casing	8.88	inch
Open hole diameter	8.5	inch
Flow rate	846	gpm
Fracture pressure equivalent density	10.6	ppg
Pore pressure equivalent density	8.4	ppg
Measured ECD at MD of 12600 ft	9.17	ppg

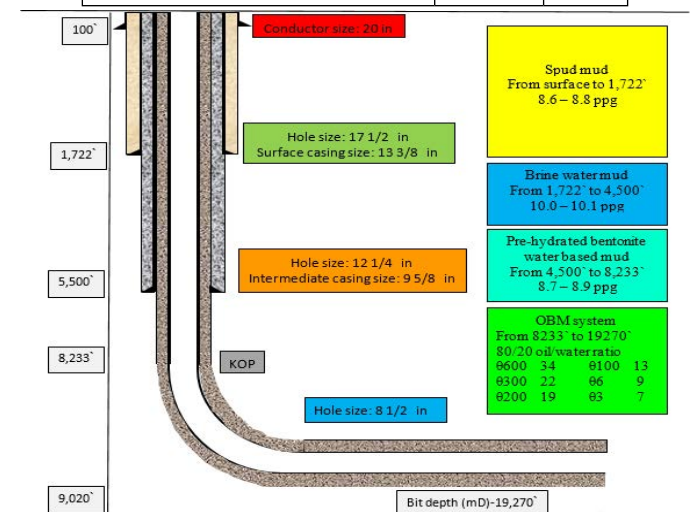


**Figure 7:** Wellbore sketch with corresponding drilling fluids.

The measurements for fluid rheology for WBM without FR, developed WBM with FR, actual OBM used in drilling this well, are mentioned in (Table 6). The fluid rheology was measured after hot rolling at 120°F. The Herschel-Bulkley model parameters ( $n$ ,  $K$ , and  $\tau_y$ ) were calculated and tabulated in table.

The  $R^2$  calculations demonstrates the accuracy of the calculated Herschel-Bulkley parameters in forecasting fluid rheology when compared to the measured fluid rheology. As, all  $R^2$  values were higher than 0.98 and proved the sufficiency of Herschel-Bulkley model to simulate actual fluid rheology.

**Table 6:** The value of Hershel-Buckley parameters for different formulated muds.

	WBM without FR	WBM with 0.50 lb/bbl FR	OBM
Shear stress at 600 rpm, DR	16	29	34
Shear stress at 300 rpm, DR	11	20	22
Shear stress at 200 rpm, DR	9	17	19
Shear stress at 100 rpm, DR	7	13	13
Shear stress at 6 rpm, DR	6	8	9
Shear stress at 3 rpm, DR	5	7	7
$\tau_y$ (lb/ft <sup>2</sup> )	5.3	7.24	7.96
n	0.94	0.77	0.88
K (lb <sub>f</sub> .S <sup>n</sup> /100 ft <sup>2</sup> )	0.016	0.11	0.06
R <sup>2</sup>	0.986	0.998	0.996

The ECD calculated using the Herschel-Bulkley model for various drilling fluids (WBM without FR, developed WBM with FR, and OBM is depicted in **(Figure 8)**. The computed ECD is based on a mud density of 8.75 ppg. To check the precision of the model employed in this study for ECD computation using the Herschel-Bulkley model, the computed ECD was juxtaposed with the measured ECD at MD of 12600 ft, as illustrated in **(Table 5)**. At MD of 12600 ft, the computed ECD was 9.16 ppg, in contrast to the measured ECD of 9.17 ppg. Consequently, the discrepancy in the calculated ECD is approximately 0.1%, underscoring the high accuracy of the model in ECD calculation. It is clear based on **(Figures 8, 9)** that the calculated ECD for WBM with FR is lower than the ECD for WBM without FR. Moreover, the ECD curve for WBM with FR closely resembles that of OBM, with the difference between ECD and static density ranging from 0.25 ppg to 0.65 ppg. This indicates that the FR is effective in minimizing ECD for WBM and exhibits ECD performance comparable to that of OBM. Besides, Using FR can be used to drill narrow windows between pore pressure and fracture pressure. Consequently, FR plays a crucial role in reducing pressure drop in the annulus and lowering the surface pump capacity requirements. Ultimately, this contributes to expanding the lateral section of horizontal wells.

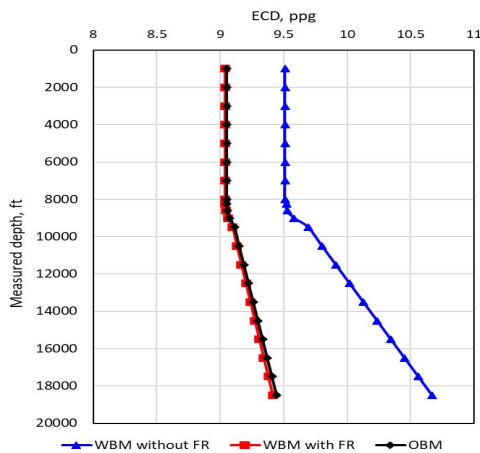


**Figure 8:** The calculated ECD for different drilling fluids using Herschel-Bulkley model.

Additionally, sensitivity analysis was conducted to determine ERW horizontal sectional limit. The target from this sensitivity analysis is to determine possibility of using the developed WBM with FR to extend horizontal section limit. The author didn't change equivalent density for both pore pressure and fracture pressure, and operating pump flow rate and kept it as 846 ppg. The open hole horizontal extension limit calculations were done

as mentioned in the modelling part using Herschel-Bulkley model at different mud densities ranged from 8.75 ppg to 10 ppg and at different eccentricity assumed values ranged from 0 to 1.

The calculations for horizontal extension limit are illustrated in **(Figures 9, 10, 11)**. These figures show that the values of horizontal section limit decrease with the increase in mud density. Also, the calculations clarify that eccentricity effect leads to increase ERW length for different formulated drilling fluids. The maximum horizontal section length drilled by using WBM formulated without FR with density 8.5 ppg was 9,000 ft, and 15000 ft when eccentricity is 0 and 1, respectively **(Figure 9)**. Besides, Fig.13 simplifies no horizontal section can be drilled with 10 ppg WBM formulated without FR. When FR added to WBM, the maximum horizontal length can be drilled by this fluid with 8.5 ppg density is 12,500 ft when eccentricity is 0 and 20,000 ft when eccentricity is 1 **(Figure 10)**. Hence, adding FR to WBM can extend horizontal limit of ERW with 3500 ft, and 7500 ft in fully concentric, and eccentric condition, respectively. On the other hand, calculations of open hole horizontal section limit by using OBM approaches those calculations from using WBM with FR as seen in **(Figure 11)**.

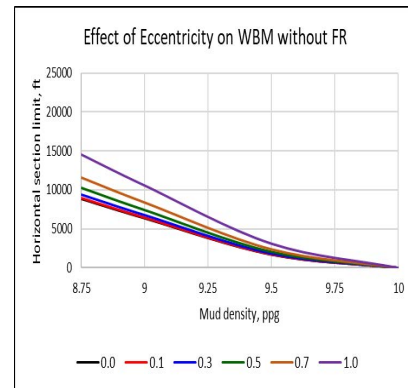


**Figure 9:** Open hole horizontal extension limit by using WBM without FR.

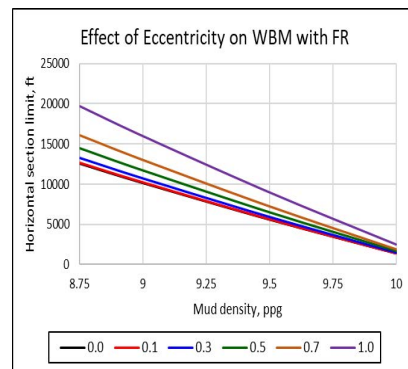


**Figure 10:** Open hole horizontal extension by using WBM with FR.

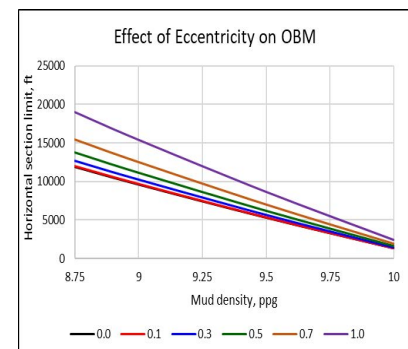


**Figure 11:** Open hole horizontal extension limit by using WBM with OBM.

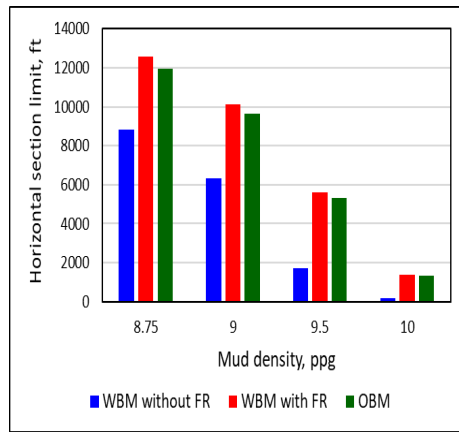


**Figure 12:** Mud density effect on concentric horizontal extension limit using different fluids.

The effect of mud density of different drilling fluids in fully concentric conditions was shown in (Figure 12). The WBM with FR has the same calculated ERW limit like OBM at all mud density and higher than ERW limit of the well drilled with WBM without FR. For instance, the maximum ERW horizontal extended limit drilled by 9 ppg WBM with FR will be 10,000 ft, while being 6,000 ft in case of WBM without FR with the same density. Subsequently, the increase in horizontal extended limit will be about 60% when FR added to WBM with 9 ppg. This means adding FR to WBM stabilizes shale and prevents shale problems, enhances thermal stability for mud rheology, reduces and control ECD, will increase drilling for horizontal ERW limit.

Another sensitivity analysis is conducted based on increase fracture pressure. The current equivalent density of fracture pressure at TVD of 9020 ft is 10.6 ppg. The new assumed values for equivalent density of fracture pressure are 11 and 12 ppg at TVD of 9020 ft. The horizontal extension limit for ERW shown in (Figure 7) was calculated using flow rate of 846 ppg and Herschel-Bulkley parameters mentioned in table 6. The results of the extension on the horizontal ERW section are graphically represented in (Figure 13). With an equivalent density for fracture pressure set at 11 ppg, the horizontal section of ERW at 8.75 ppg is anticipated to extend to 15000 ft when utilizing OBM and developed WBM with FR. Conversely, the extension reduces to 11000 ft when using WBM without FR. Conversely, implementing 8.75 ppg WBM with 0.5 lb/bbl FR is projected to extend the open hole horizontal section to 25000ft when the equivalent density of fracture pressure is 12 ppg.

Consequently, the incorporation of FR into WBM is expected to result in an additional drilling depth of around 4000 ft compared to using WBM without FR. This addition of FR to WBM aims to decrease hydraulic friction losses, minimize ECD, and extend the horizontal section of ERW.

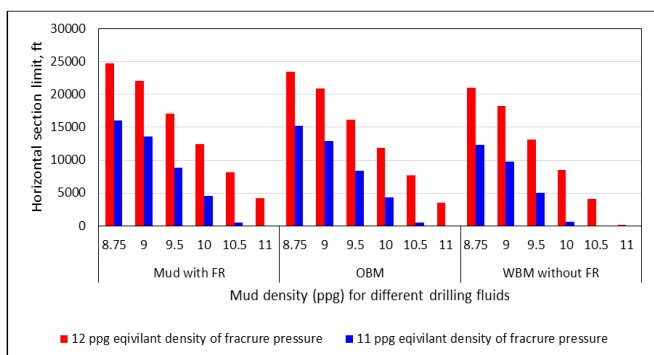


**Figure13:** Horizontal section limit at different fracture pressures.

### 5. Conclusion

This paper focused experimentally on formulation high performance WBM using FR. It concentrated on how the developed WBM with FR to inhibit shale problems, resist thermal degradation, minimize ECD, approach OBM performance in Permian Basin. Modelling annular pressure losses using Hershel-Bulkley rheological model is also used to determine increase in open hole extensional limit of the ERW drilled by the formulated OBM and WBM with FR. The following conclusions are drawn from the study:

- The formulated WBM with FR resist thermal mud degradation up to 180° F.
- Zeta potential, and shale dispersion test prove the developed WBM with FR is efficient to stabilize shale and prevent shale swelling and dispersion.
- Adding 0.5 lb/bbl FR to WBM increased shale recovery for Wolfcamp shale cuttings to 98%
- FR is working as a shale inhibitor by encapsulating clay surface and KCl salt enhanced this encapsulation through bridging.
- The model presented in this paper provides more precise predictions for ECD and consequently accurate estimation to the open hole horizontal section for ERW extension.
- The calculated ECD using Herschel-Bulkley model for the developed WBM is identical as OBM and more than static density of 8.75 ppg by (0.25 ppg to 0.65 ppg)
- The incorporation of FR into WBM enhances the capacity to prolong the horizontal section of ERW by reducing annular pressure loss frictions.
- The formulated WBM with FR could be used to replace OBM when drilling ERW lateral section in Wolfcamp formation within the Permian basin.

### Nomenclature

$P_{bh}$	Bottom hole pressure, psi	$L_v$	The vertical section length, ft
$P_f$	Fracture pressure, psi	$L_h$	The horizontal section limit, ft
$P_{hy}$	Mud hydrostatic pressure, psi	$\rho_m$	Mud density
$\Delta P_v$	Annular pressure loss in vertical section, psi	$\rho_f$	The equivalent density of the formation fracture pressure, ppg
$\Delta P_h$	Annular pressure loss in horizontal section, psi	$\Delta P_{ds}$	Annular pressure loss in short deviated section, psi
$\Delta P_{dl}$	Annular pressure loss in long deviated section, psi	$d_o$	The casing inner diameter or wellbore diameter
$f_a$	The annular friction factor	$d_i$	The drill pipe outer diameter
$R_{lam}$	Laminar eccentric coefficient	ECD	Equivalent circulation density
$R_{turb}$	Turbulent eccentric coefficient	q	Mud flow rate
$v$	Average fluid annular velocity	KOP	Kick off Point
XC	Xanthan Gum polymer	PAC	Polyanionic cellulose
ppg	Pound per gallon	Lb/bbl	Pound per barrel
DR	Dial Reading	lbf	Pound force

## References

1. Tan Y, Li H, Zhou X, et al. Inflow characteristics of horizontal wells in sulfur gas reservoirs: A comprehensive experimental investigation. *Fuel*. 2019;238:267-274.
2. Lubrecht LMD. Horizontal directional drilling: a green and sustainable technology for site remediation. *Env Sci Tech* 2012;46(5):2484-2489.
3. Okon AN. Water Coning Prediction: An evaluation of horizontal well correlations. *Eng and App Sci*. 2018.
4. Chen X, Gao D. The Maximum-Allowable Well Depth While Performing Ultra-Extended-Reach Drilling from Shallow Water to Deepwater Target. *SPE J*. 2018;23:224-236.
5. Chamat E, Cuadros G, Trejo E, et al. Performance Step Change in Shallow Extended Reach Wells in Venezuela Enables Drilling Optimization and Increased Heavy Oil Production. In *Proceedings of the SPE Canada Heavy Oil Technical Conference*, Calgary, AB, Canada. 2015;9-11.
6. Gupta, Vishwas PYFR, Angel H, et al. Expanding the Extended Reach Envelope at Chayvo Field, Sakhalin Island. Paper presented at the IADC/SPE Drilling Conference and Exhibition, Fort Worth, Texas, USA. 2014.
7. Yeung J, Li J, Lee J, Guo X. Evaluation of Lubricants Performance for Coiled Tubing Application in Extended Reach Well. Paper Presented at the SPE/ICoTA Coiled Tubing and Well Intervention Conference and Exhibition, Houston, Texas, USA. 2017.
8. Li X, Gao D, Lu B, Zeng Y, Ding S, Zhou S. A prediction model of the shortest drilling time for horizontal section in extended-reach well. *J Petro Sci and Eng*. 2019.
9. Sabeh K E, Gaurina-Međimurec N, Mijić P, Medved' I, Pašić B. Extended-Reach Drilling (ERD)-The main problems and current achievements. *App Sci*. 2023;13(7):4112.
10. Morrison A, Serov N A, Fahmy A. Completing Ultra Extended-Reach Wells: Overcoming the Torque and Drag Constraints of Brine. *ADIPEC*. 2019.
11. Metwally M, Nguyen T, Wiggins H, et al. Evaluations of Polyacrylamide Water-Based Drilling Fluids for Horizontal Drilling in the Shaly Wolfcamp Formation. *SPE J*. 2023;28:1744-1759.
12. Cameron CA. Drilling fluids design and management for extended reach drilling. *All Days*. 2001;22-24.
13. John, Tellez Diego, Neel, Randy, et al. Unconventional Drilling in the New Mexico Delaware Basin Case History. *Proc. IADC/SPE Drilling Conference and Exhibition*. 2018;6-8.
14. Njuguna J, Siddique S, K wroffie L B, et al. The fate of waste drilling fluids from oil & gas industry activities in the exploration and production operations. *Waste Manag*. 2022;139:362-380.
15. Saleh TA. Advanced trends of shale inhibitors for enhanced properties of water-based drilling fluid. *Upstream Oil Gas Techn*. 2022;8:100069.
16. Yuan J, Yu Y, Liu S, et al. Technical difficulties in the cementing of horizontal shale gas wells in Weiyuan block and the countermeasures. *Nat Gas Indus B*. 2016;3(3):260-268.
17. Metwally M, Nguyen, T. Effectiveness of Shale Inhibition by Anionic and Cationic Polyacrylamide Copolymers in Water Based Mud. The AADE National Technical Conference and Exhibition, The Bush Convention Center, Midland, Texas. 2023.
18. Varnaseri M, Peyghambarzadeh SM. The effect of polyacrylamide drag reducing agent on friction factor and heat transfer coefficient in laminar, transition and turbulent flow regimes in circular pipes with different diameters. *Int J Heat Mass Tran*. 2020;154:119815.
19. Aften C, Watson W. Improved Friction Reducer for Hydraulic Fracturing, Presented at the SPE Hydraulic Fracturing Technology Conference in Woodlands, TX. *SPE*. 2009;118747.
20. Ibrahim A, Nasr-El-Din HA, Rabie, Al, et al. A New Friction-Reducing Agent for Slickwater-Fracturing Treatments. *SPE Prod Oper*. 2018;33(3):583-595.
21. Khalil MF, Kassab SZ, Elmiligui AA, Naoum FA. Applications of drag-reducing polymers in sprinkler irrigation systems: Sprinkler head performance, *J Irrig Drain Eng*. 2002;128(3):147-152.
22. Figueredo RCR, Sabadini E. Firefighting foam stability: the effect of the drag reducer poly (ethylene) oxide, *Colloids Surf. A Physico chem Eng Asp*. 2003;215(1-3):77-86.
23. Kotenko M, Oskarsson H, Bojesen C, Nielsen MP. An experimental study of the drag reducing surfactant for district heating and cooling. *Energy*. 2019;178:72-78.
24. Edomwonyi-Otu LC, Adelokun DO. Effect of heavy molecular weight polymer on quality of drinking water, *Mater. Today Common*. 2018;15:337-343.
25. Bradshaw P. Possible origin of Prandtl's mixing-length theory. *Nature*. 1974;249(5453):135-136.
26. Nguyen T, Romero B, Vinson E, Wiggins H. Effect of salt on the performance of drag reducers in slickwater fracturing fluids. *J Petrol Sci Eng* 2018;163:590-599.
27. Diamond P, Harvey J, Katz J, Nelson D, Steinhardt P. Drag reduction by polymer additives. In: *JASON the MITRE Corporation*. JSR. 1992;89-720.
28. Douglas F. Wolfcampian Development of the Nose of the Eastern Shelf of the Midland Basin, Glasscock, Sterling, and Reagan Counties, Texas. *Theses and Dissertations*. 2008;1555.
29. Forrest James, Tiejun Zhu, Hongjie Xiong, Yogashri Pradhan. The Effect of Initial Conditions and Fluid PVT Properties on Unconventional Oil and Gas Recoveries in the Wolfcamp Formation in the Midland Basin. Paper presented at the SPE/AAPG/SEG Unconventional Resources Technology Conference, Houston, Texas, USA. 2018.
30. Baker Hughes Rig Count. Baker Hughes Rig Count. 2023.
31. American Petroleum Institute (API). Recommended Practice for Field Testing Water-based Drilling Fluids. *API RP 13B-1*, 5th Edition. 2019.
32. Ahmed HM, Kamal MS, Al-Harhi MA. Polymeric and low molecular weight shale inhibitors: A review. *Fuel*. 2019;251:187-217.
33. Jain R, Mahto V, Sharma V. Evaluation of polyacrylamide-grafted-polyethylene glycol/silica nanocomposite as potential additive in water-based drilling mud for reactive shale formation. *J Natural Gas Sci Eng*. 2015;26:526-537.
34. Metwally M, Nguyen TD, Wiggins H, et al. Experimental lab approach for water-based drilling fluid using polyacrylamide friction reducers to drill extended horizontal wells. *J Petro Sci and Eng*. 2022;212:110132.
35. Deli Gao, Chengjin Tan, Haixiong Tang. Limit analysis of extended reach drilling in South China Sea. *Petro Sci*. 2009;6(2):166-171.
36. Folan JA, Anawe PAL, Abioye PO, Elehinafe, FB. Selecting the Most Appropriate Model for Rheological Characterization of Synthetic Based Drilling Mud. *Inter J App Eng Res*. 2016;12(18):7614-7629.
37. Guo B, Liu G. Applied Drilling Circulation Systems: hydraulics, calculations, and models. 2011.
38. Xin Li, Deli Gao, Yingcao Zhou, et al. General approach for the calculation and optimal control of the extended-reach limit in horizontal drilling based on the mud weight window. *J Nat Gas Sci Eng*. 2016;35:964-979.
39. Erge Oney, Ozbayoglu, Evren M, et al. The effects of drill string eccentricity, rotation and buckling configurations on annular frictional pressure losses while circulating yield power law fluids. In: *Paper SPE-167950-MS Presented at the 2014 IADC/SPE Drilling Conference and Exhibition Held in Fort Worth, Texas, USA, 4e6 March 2014*.
40. Bailey WJ, Peden J. A generalized and consistent pressure drop and flow regime transition model for drilling hydraulics. *SPE Drilling & Completion*. 2000;15(1):44-56.

41. Mpofu P, Addai-Mensah J, Ralston J. Temperature influence of nonionic polyethylene oxide and anionic polyacrylamide on flocculation and dewatering behavior of kaolinite dispersions. *J Colloid Interface Sci.* 2004;145-156.
42. Ghanbari S, Kazemzadeh E, Soleymani M, Naderifar, A. A facile method for synthesis and dispersion of silica nanoparticles in water-based drilling fluid. *Colloid Poly Sci.* 2015;294(2):381-388.
43. Alberty MW, McLean. Fracture gradients in depleted reservoirs - drilling wells in latereservoir life. *All Days.* 2001.